Fermi National Accelerator Laboratory

FERMILAB-Pub-98/263-E
CDF

Search for the Decays B_s^0, $B_d^0 \to e^{\pm}\mu^{\mp}$ and Pati-Salam Leptoquarks

F. Abe et al.
The CDF Collaboration

Fermi National Accelerator Laboratory
P.O. Box 500, Batavia, Illinois 60510

August 1998

Submitted to *Physical Review Letters*

Operated by Universities Research Association Inc. under Contract No. DE-AC02-76CH03000 with the United States Department of Energy

Disclaimer

Distribution

Search for the Decays $B_s^0, B_d^0 \to e^{\pm}\mu^{\mp}$ and Pati-Salam Leptoquarks

(August 25, 1998)

F. Abe,[17] H. Akimoto,[39] A. Akopian,[31] M. G. Albrow,[7] A. Amadon,[5] S. R. Amendolia,[27] D. Amidei,[20] J. Antos,[33] S. Aota,[37] G. Apollinari,[31] T. Arisawa,[39] T. Asakawa,[37] W. Ashmanskas,[18] M. Atac,[7] P. Azzi-Bacchetta,[25] N. Bacchetta,[25] S. Bagdasarov,[31] M. W. Bailey,[22] P. de Barbaro,[30] A. Barbaro-Galtieri,[18] V. E. Barnes,[29] B. A. Barnett,[15] M. Barone,[9] G. Bauer,[19] T. Baumann,[11] F. Bedeschi,[27] S. Behrends,[3] S. Belforte,[27] G. Bellettini,[27] J. Bellinger,[40] D. Benjamin,[35] J. Bensinger,[3] A. Beretvas,[7] J. P. Berge,[7] J. Berryhill,[5] S. Bertolucci,[9] S. Bettelli,[27] B. Bevensee,[26] A. Bhatti,[31] K. Biery,[7] C. Bigongiari,[27] M. Binkley,[7] D. Bisello,[25] R. E. Blair,[1] C. Blocker,[3] K. Bloom,[20] S. Blusk,[30] A. Bodek,[30] W. Bokhari,[26] G. Bolla,[29] Y. Bonushkin,[4] D. Bortoletto,[29] J. Boudreau,[28] L. Breccia,[2] C. Bromberg,[21] N. Bruner,[22] R. Brunetti,[2] E. Buckley-Geer,[7] H. S. Budd,[30] K. Burkett,[11] G. Busetto,[25] A. Byon-Wagner,[7] K. L. Byrum,[1] M. Campbell,[20] A. Caner,[27] W. Carithers,[18] D. Carlsmith,[40] J. Cassada,[30] A. Castro,[25] D. Cauz,[36] A. Cerri,[27] P. S. Chang,[33] P. T. Chang,[33] H. Y. Chao,[33] J. Chapman,[20] M. -T. Cheng,[33] M. Chertok,[34] G. Chiarelli,[27] C. N. Chiou,[33] F. Chlebana,[7] L. Christofek,[13] R. Cropp,[14] M. L. Chu,[33] S. Cihangir,[7] A. G. Clark,[10] M. Cobal,[27] E. Cocca,[27] M. Contreras,[5] J. Conway,[32] J. Cooper,[7] M. Cordelli,[9] D. Costanzo,[27] C. Couyoumtzelis,[10] D. Cronin-Hennessy,[6] R. Culbertson,[5] D. Dagenhart,[38] T. Daniels,[19] F. DeJongh,[7] S. Dell'Agnello,[9] M. Dell'Orso,[27] R. Demina,[7] L. Demortier,[31] M. Deninno,[2] P. F. Derwent,[7] T. Devlin,[32] J. R. Dittmann,[6] S. Donati,[27] J. Done,[34] T. Dorigo,[25] N. Eddy,[13] K. Einsweiler,[18] J. E. Elias,[7] R. Ely,[18] E. Engels, Jr.,[28] W. Erdmann,[7] D. Errede,[13] S. Errede,[13] Q. Fan,[30] R. G. Feild,[41] Z. Feng,[15] C. Ferretti,[27] I. Fiori,[2] B. Flaugher,[7] G. W. Foster,[7] M. Franklin,[11] J. Freeman,[7] J. Friedman,[19] H. Frisch,[5] Y. Fukui,[17] S. Gadomski,[14] S. Galeotti,[27] M. Gallinaro,[26] O. Ganel,[35] M. Garcia-Sciveres,[18] A. F. Garfinkel,[29] C. Gay,[41] S. Geer,[7] D. W. Gerdes,[15] P. Giannetti,[27] N. Giokaris,[31] P. Giromini,[9] G. Giusti,[27] M. Gold,[22] A. Gordon,[11] A. T. Goshaw,[6] Y. Gotra,[28] K. Goulianos,[31] H. Grassmann,[36] L. Groer,[32] C. Grosso-Pilcher,[5] G. Guillian,[20] J. Guimaraes da Costa,[15] R. S. Guo,[33] C. Haber,[18] E. Hafen,[19] S. R. Hahn,[7] R. Hamilton,[11] T. Handa,[12] R. Handler,[40] F. Happacher,[9] K. Hara,[37] A. D. Hardman,[29] R. M. Harris,[7] F. Hartmann,[16] J. Hauser,[4] E. Hayashi,[37] J. Heinrich,[26] W. Hao,[35] B. Hinrichsen,[14] K. D. Hoffman,[29] M. Hohlmann,[5] C. Holck,[26] R. Hollebeek,[26] L. Holloway,[13] Z. Huang,[20] B. T. Huffman,[28] R. Hughes,[23] J. Huston,[21] J. Huth,[11] H. Ikeda,[37] M. Incagli,[27] J. Incandela,[7] G. Introzzi,[27] J. Iwai,[39] Y. Iwata,[12] E. James,[20] H. Jensen,[7] U. Joshi,[7] E. Kajfasz,[25] H. Kambara,[10] T. Kamon,[34] T. Kaneko,[37] K. Karr,[38] H. Kasha,[41] Y. Kato,[24] T. A. Keaffaber,[29] K. Kelley,[19]

R. D. Kennedy,[7] R. Kephart,[7] D. Kestenbaum,[11] D. Khazins,[6] T. Kikuchi,[37] B. J. Kim,[27] H. S. Kim,[14] S. H. Kim,[37] Y. K. Kim,[18] L. Kirsch,[3] S. Klimenko,[8] D. Knoblauch,[16] P. Koehn,[23] A. Köngeter,[16] K. Kondo,[37] J. Konigsberg,[8] K. Kordas,[14] A. Korytov,[8] E. Kovacs,[1] W. Kowald,[6] J. Kroll,[26] M. Kruse,[30] S. E. Kuhlmann,[1] E. Kuns,[32] K. Kurino,[12] T. Kuwabara,[37] A. T. Laasanen,[29] S. Lami,[27] S. Lammel,[7] J. I. Lamoureux,[3] M. Lancaster,[18] M. Lanzoni,[27] G. Latino,[27] T. LeCompte,[1] S. Leone,[27] J. D. Lewis,[7] M. Lindgren,[4] T. M. Liss,[13] J. B. Liu,[30] Y. C. Liu,[33] N. Lockyer,[26] O. Long,[26] C. Loomis,[32] M. Loreti,[25] D. Lucchesi,[27] P. Lukens,[7] S. Lusin,[40] J. Lys,[18] K. Maeshima,[7] P. Maksimovic,[11] M. Mangano,[27] M. Mariotti,[25] J. P. Marriner,[7] G. Martignon,[25] A. Martin,[41] J. A. J. Matthews,[22] P. Mazzanti,[2] K. McFarland,[30] P. McIntyre,[34] P. Melese,[31] M. Menguzzato,[25] A. Menzione,[27] E. Meschi,[27] S. Metzler,[26] C. Miao,[20] T. Miao,[7] G. Michail,[11] R. Miller,[21] H. Minato,[37] S. Miscetti,[9] M. Mishina,[17] S. Miyashita,[37] N. Moggi,[27] E. Moore,[22] Y. Morita,[17] A. Mukherjee,[7] T. Muller,[16] P. Murat,[27] S. Murgia,[21] M. Musy,[36] H. Nakada,[37] T. Nakaya,[5] I. Nakano,[12] C. Nelson,[7] D. Neuberger,[16] C. Newman-Holmes,[7] C.-Y. P. Ngan,[19] L. Nodulman,[1] A. Nomerotski,[8] S. H. Oh,[6] T. Ohmoto,[12] T. Ohsugi,[12] R. Oishi,[37] M. Okabe,[37] T. Okusawa,[24] J. Olsen,[40] C. Pagliarone,[27] R. Paoletti,[27] V. Papadimitriou,[35] S. P. Pappas,[41] N. Parashar,[27] A. Parri,[9] J. Patrick,[7] G. Pauletta,[36] M. Paulini,[18] A. Perazzo,[27] L. Pescara,[25] M. D. Peters,[18] T. J. Phillips,[6] G. Piacentino,[27] M. Pillai,[30] K. T. Pitts,[7] R. Plunkett,[7] A. Pompos,[29] L. Pondrom,[40] J. Proudfoot,[1] F. Ptohos,[11] G. Punzi,[27] K. Ragan,[14] D. Reher,[18] M. Reischl,[16] A. Ribon,[25] F. Rimondi,[2] L. Ristori,[27] W. J. Robertson,[6] A. Robinson,[14] T. Rodrigo,[27] S. Rolli,[38] L. Rosenson,[19] R. Roser,[13] T. Saab,[14] W. K. Sakumoto,[30] D. Saltzberg,[4] A. Sansoni,[9] L. Santi,[36] H. Sato,[37] P. Schlabach,[7] E. E. Schmidt,[7] M. P. Schmidt,[41] A. Scott,[4] A. Scribano,[27] S. Segler,[7] S. Seidel,[22] Y. Seiya,[37] F. Semeria,[2] T. Shah,[19] M. D. Shapiro,[18] N. M. Shaw,[29] P. F. Shepard,[28] T. Shibayama,[37] M. Shimojima,[37] M. Shochet,[5] J. Siegrist,[18] A. Sill,[35] P. Sinervo,[14] P. Singh,[13] K. Sliwa,[38] C. Smith,[15] F. D. Snider,[15] J. Spalding,[7] T. Speer,[10] P. Sphicas,[19] F. Spinella,[27] M. Spiropulu,[11] L. Spiegel,[7] L. Stanco,[25] J. Steele,[40] A. Stefanini,[27] R. Ströhmer,[7a] J. Strologas,[13] F. Strumia, [10] D. Stuart,[7] K. Sumorok,[19] J. Suzuki,[37] T. Suzuki,[37] T. Takahashi,[24] T. Takano,[24] R. Takashima,[12] K. Takikawa,[37] M. Tanaka,[37] B. Tannenbaum,[4] F. Tartarelli,[27] W. Taylor,[14] M. Tecchio,[20] P. K. Teng,[33] Y. Teramoto,[24] K. Terashi,[37] S. Tether,[19] D. Theriot,[7] T. L. Thomas,[22] R. Thurman-Keup,[1] M. Timko,[38] P. Tipton,[30] A. Titov,[31] S. Tkaczyk,[7] D. Toback,[5] K. Tollefson,[30] A. Tollestrup,[7] H. Toyoda,[24] W. Trischuk,[14] J. F. de Troconiz,[11] S. Truitt,[20] J. Tseng,[19] N. Turini,[27] T. Uchida,[37] F. Ukegawa,[26] J. Valls,[32] S. C. van den Brink,[28] S. Vejcik, III,[20] G. Velev,[27] R. Vidal,[7] R. Vilar,[7a] D. Vucinic,[19] R. G. Wagner,[1] R. L. Wagner,[7] J. Wahl,[5] N. B. Wallace,[27] A. M. Walsh,[32] C. Wang,[6] C. H. Wang,[33] M. J. Wang,[33] A. Warburton,[14] T. Watanabe,[37] T. Watts,[32] R. Webb,[34] C. Wei,[6] H. Wenzel,[16] W. C. Wester, III,[7] A. B. Wicklund,[1]

E. Wicklund,[7] R. Wilkinson,[26] H. H. Williams,[26] P. Wilson,[7] B. L. Winer,[23] D. Winn,[20] D. Wolinski,[20] J. Wolinski,[21] S. Worm,[22] X. Wu,[10] J. Wyss,[27] A. Yagil,[7] W. Yao,[18] K. Yasuoka,[37] G. P. Yeh,[7] P. Yeh,[33] J. Yoh,[7] C. Yosef,[21] T. Yoshida,[24] I. Yu,[7] A. Zanetti,[36] F. Zetti,[27] and S. Zucchelli[2]

(CDF Collaboration)

[1] *Argonne National Laboratory, Argonne, Illinois 60439*

[2] *Istituto Nazionale di Fisica Nucleare, University of Bologna, I-40127 Bologna, Italy*

[3] *Brandeis University, Waltham, Massachusetts 02254*

[4] *University of California at Los Angeles, Los Angeles, California 90024*

[5] *University of Chicago, Chicago, Illinois 60637*

[6] *Duke University, Durham, North Carolina 27708*

[7] *Fermi National Accelerator Laboratory, Batavia, Illinois 60510*

[8] *University of Florida, Gainesville, Florida 32611*

[9] *Laboratori Nazionali di Frascati, Istituto Nazionale di Fisica Nucleare, I-00044 Frascati, Italy*

[10] *University of Geneva, CH-1211 Geneva 4, Switzerland*

[11] *Harvard University, Cambridge, Massachusetts 02138*

[12] *Hiroshima University, Higashi-Hiroshima 724, Japan*

[13] *University of Illinois, Urbana, Illinois 61801*

[14] *Institute of Particle Physics, McGill University, Montreal H3A 2T8, and University of Toronto, Toronto M5S 1A7, Canada*

[15] *The Johns Hopkins University, Baltimore, Maryland 21218*

[16] *Institut für Experimentelle Kernphysik, Universität Karlsruhe, 76128 Karlsruhe, Germany*

[17] *National Laboratory for High Energy Physics (KEK), Tsukuba, Ibaraki 305, Japan*

[18] *Ernest Orlando Lawrence Berkeley National Laboratory, Berkeley, California 94720*

[19] *Massachusetts Institute of Technology, Cambridge, Massachusetts 02139*

[20] *University of Michigan, Ann Arbor, Michigan 48109*

[21] *Michigan State University, East Lansing, Michigan 48824*

[22] *University of New Mexico, Albuquerque, New Mexico 87131*

[23] *The Ohio State University, Columbus, Ohio 43210*

[24] *Osaka City University, Osaka 588, Japan*

[25] *Universita di Padova, Istituto Nazionale di Fisica Nucleare, Sezione di Padova, I-35131 Padova, Italy*

[26] *University of Pennsylvania, Philadelphia, Pennsylvania 19104*

[27] *Istituto Nazionale di Fisica Nucleare, University and Scuola Normale Superiore of Pisa, I-56100 Pisa, Italy*

[28] *University of Pittsburgh, Pittsburgh, Pennsylvania 15260*

[29] *Purdue University, West Lafayette, Indiana 47907*

[30] *University of Rochester, Rochester, New York 14627*

[31] *Rockefeller University, New York, New York 10021*

[32] *Rutgers University, Piscataway, New Jersey 08855*

[33] *Academia Sinica, Taipei, Taiwan 11530, Republic of China*

[34] *Texas A&M University, College Station, Texas 77843*

[35] *Texas Tech University, Lubbock, Texas 79409*

[36] *Istituto Nazionale di Fisica Nucleare, University of Trieste/ Udine, Italy*

[37] *University of Tsukuba, Tsukuba, Ibaraki 315, Japan*

[38] *Tufts University, Medford, Massachusetts 02155*

[39] *Waseda University, Tokyo 169, Japan*

[40] *University of Wisconsin, Madison, Wisconsin 53706*

[41] *Yale University, New Haven, Connecticut 06520*

We have searched for the decays $B_s^0 \to e^{\pm}\mu^{\mp}$ and $B_d^0 \to e^{\pm}\mu^{\mp}$ using a 102 pb^{-1} data sample of $p\bar{p}$ collisions at $\sqrt{s} = 1.8$ TeV collected with the Collider Detector at Fermilab. We set upper limits on the branching fractions of $\mathcal{B}(B_s^0 \to e^{\pm}\mu^{\mp}) < 6.1(8.2) \times 10^{-6}$ and $\mathcal{B}(B_d^0 \to e^{\pm}\mu^{\mp}) < 3.5(4.5) \times 10^{-6}$ at 90(95)% confidence level. Using these limits, we set lower bounds on the corresponding Pati-Salam leptoquark masses and find that $\mathrm{M_{LQ}}(B_s^0) > 20.7(19.3)$ TeV/c^2 and $\mathrm{M_{LQ}}(B_d^0) > 21.7(20.4)$ TeV/c^2 at 90(95)% confidence level.

14.40.Nd, 13.20.He, 12.60.-i

Within the Standard Model the decays $B_s^0 \to e^\pm\mu^\mp$ and $B_d^0 \to e^\pm\mu^\mp$ are forbidden by lepton flavor conservation; observation of either of these decays would be evidence for new physics. In particular the assumption of a local gauge symmetry between quarks and leptons leads to the prediction of a new force of nature that mediates transitions between quarks and leptons. One of the simplest models that incorporates this idea is the Pati-Salam model [1] based on the group $SU(4)_c$ where the lepton number is the fourth "color." At some high-energy scale, the group $SU(4)_c$ is spontaneously broken to $SU(3)_c$, liberating the leptons from the influence of the strong interaction and breaking the symmetry between quarks and leptons. This model predicts heavy spin-one gauge bosons called Pati-Salam leptoquarks (LQ) that carry both color and lepton quantum numbers. The lepton and quark components are not necessarily from the same generation and can mediate the decays $B_s^0 \to e^\pm\mu^\mp$ and $B_d^0 \to e^\pm\mu^\mp$ [2] [3]. The decay $B_s^0 \to e^\pm\mu^\mp$ probes two types of LQ: (1) a leptoquark coupling the electron with the b-quark and the muon with the s-quark, (2) a leptoquark coupling the electron with the s-quark and the muon with the b-quark. Similarly, $B_d^0 \to e^\pm\mu^\mp$ probes two different types of LQ.

The current best limits on the branching fractions $\mathcal{B}(B_s^0 \to e^\pm\mu^\mp)$ and $\mathcal{B}(B_d^0 \to e^\pm\mu^\mp)$ are $4.1(5.3) \times 10^{-5}$ at 90(95)% confidence level (C.L.) and 5.9×10^{-6} at 90% C.L., set by the L3 [4] and CLEO [5] collaborations, respectively. We present more stringent limits on both $\mathcal{B}(B_s^0 \to e^\pm\mu^\mp)$ and $\mathcal{B}(B_d^0 \to e^\pm\mu^\mp)$, and limits on the corresponding leptoquark masses $M_{LQ}(B_s^0)$ and $M_{LQ}(B_d^0)$, using a data sample of 102 pb^{-1} of $p\bar{p}$ collisions at $\sqrt{s} = 1.8$ TeV collected during 1992-1995 with the Collider Detector at Fermilab (CDF).

The CDF detector has been described in detail elsewhere [6]. We briefly describe here those aspects of the detector relevant to this analysis. The tracking system is immersed in a 1.4 T solenoidal magnetic field. The innermost tracking device is a silicon micro-strip vertex detector (SVX) [7] that provides spatial measurements in the r-ϕ [8] plane. The impact parameter [9] resolution of the SVX is $13 + 40/p_T$ μm where p_T is the transverse momentum of the track in GeV/c.

Surrounding the SVX is the central tracking chamber (CTC), which extends out to a radius of 1.3 m and covers the pseudorapidity interval $|\eta| < 1.0$. Combined, the CTC and SVX provide a p_T resolution of $\delta p_T/p_T = \sqrt{(0.9p_T)^2 + (6.6)^2} \times 10^{-3}$, where p_T is in GeV/c. Electromagnetic (CEM) and hadronic (CHA) calorimeters covering $|\eta| < 1.1$ are located outside the solenoid. A layer of proportional chambers (CES) is embedded in the CEM near shower maximum and measures the shower profile and position. Three muon subsystems in the central region are used. The CMU system is located outside the hadron calorimeter and covers the region $|\eta| < 0.6$. The CMP system is located outside the CMU

behind additional steel absorber. Finally, the CMX system extends the coverage up to pseudorapidity $|\eta| = 1.0$.

A three-level trigger selects the $e\mu$ candidate events used in this analysis. To be able to predict the signal rate, we require that our candidates satisfy specific triggers at each level. At Level 1 we require the presence of a track-segment in the CMU or the CMX and an electromagnetic energy deposit (EM cluster) in the CEM. At Level 2 we require that the muon track and the EM cluster have matching charged tracks in the CTC found with the Central Fast Track processor [10]. The combined efficiency of the Level 1 and Level 2 trigger for finding CMU muons rises from 80% at $p_T(\mu) = 3.0$ GeV/c to a plateau efficiency of 87% at $p_T(\mu) = 3.3$ GeV/c. The combined efficiency of the Level 1 and Level 2 trigger for finding CMX muons rises from 50% at $p_T(\mu) = 3.0$ GeV/c to a plateau efficiency of 70% at $p_T(\mu) = 5.0$ GeV/c. The combined efficiency of the Level 1 and Level 2 trigger for finding electrons rises from 15% at $E_T(e) = 5.0$ GeV to to a plateau efficiency of 90% for $E_T(e) > 6.5$ GeV. The Level 3 software trigger requires the presence of a CEM electron with $p_T(e) > 3$ GeV/c and $E_T(e) > 5$ GeV and the presence of a muon with $p_T(\mu) > 3.0$ GeV/c in the CMU or CMX (1992-1993 run) or with $p_T(\mu) > 2.5$ GeV/c in the CMU+CMP or CMX (1994-1995 run).

The signature of the signal is an isolated oppositely charged $e\mu$ pair with an invariant mass consistent with a B meson, where B denotes B_s^0 or B_d^0 in this letter. The $e\mu$ invariant mass ($m_{e\mu}$) is calculated after constraining the two tracks to come from a common point in space. Candidates failing the fit procedure are discarded. Fig. 1 shows the $m_{e\mu}$distribution for candidates with $5 < m_{e\mu} < 6$ GeV/c^2. The distribution is flat indicating a substantial level of combinatorial background. We reduce the background by applying the proper decay length (λ), pointing angle ($\Delta\varphi$) and isolation (I) requirements, which are described below. Table I summarizes the acceptance, trigger efficiencies and the efficiencies of the offline analysis requirements.

We use a Monte Carlo simulation to estimate the acceptance listed in row 1 of Table I. We generate b quarks according to a next-to-leading order QCD calculation [11] with minimum b-quark $p_T > 5.5$ GeV/c and rapidity $|y(b)| < 1.3$. We use the normalization scale $\mu_0 = \sqrt{m_b^2 + p_T^2}$, a b-quark mass $m_b = 4.75$ GeV/c^2, and the $MRSD_0$ parton distribution functions [12]. The b quarks are fragmented into B mesons using the Peterson parameterization [13] with the fragmentation parameter value of 0.006. The B mesons are forced to decay into $e\mu$. The response of the CDF detector, including the triggers, is then simulated. The acceptance is normalized to B mesons with $p_T(B) > 6$ GeV/c and rapidity $|y(B)| < 1.0$ for which the production cross section is measured [14]. The acceptance includes the geometric acceptance as well as the kinematic requirements: $p_T(\mu) > 3.0$ GeV/c, $E_T(e) > 5$ GeV, and $p_T(e\mu) > 6.0$

GeV/c, where $\mathrm{p_T}(e\mu)$ is the transverse momentum of the $e\mu$ pair. The overall trigger efficiency is 37.2% for signal events within the geometrical and kinematical acceptance described above. This overall efficiency includes a prescale factor of 65%. The efficiency of reconstructing a track in the CTC (CTC track) has been estimated by embedding two Monte Carlo generated tracks into real data J/ψ events [15].

Muon candidates are selected as follows: the separation between the track in the muon chamber and the extrapolated CTC track is calculated in both the transverse and longitudinal planes. In each view, the difference is required to be less than 3.0 standard deviations (σ), where σ accounts for multiple scattering and measurement uncertainties. Electrons are identified by requiring that the longitudinal profile is consistent with an electron shower, i.e., small leakage in the CHA. The lateral shower profiles as measured with the CEM and CES are required to be consistent with test beam data. The CTC track is required to match the position of the calorimeter shower. Further details on electron identification are described in [16]. The efficiencies of the electron and muon selection criteria are measured using $J/\psi \to e^+e^-$ and $J/\psi \to \mu^+\mu^-$ data, respectively.

We exploit the long lifetime of B mesons to reject short-lived combinatorial background. This requires a precise measurement of the B meson decay length. For this reason, both the electron and muon are required to be reconstructed in the SVX, with hits in at least 3 of the 4 layers. The uncertainty on the transverse decay length, $L_{xy} = \frac{\vec{l}_{xy}\cdot\vec{\mathrm{p}}_\mathrm{T}(e\mu)}{\mathrm{p_T}(e\mu)}$, is required to be < 200 μm, where $\vec{l}_{xy}$ is the vector pointing from the primary vertex (the interaction point) to the secondary vertex (the reconstructed decay position) in the transverse plane, and $\vec{\mathrm{p}}_\mathrm{T}(e\mu)$ is the transverse momentum vector of the $e\mu$-pair. The mean uncertainty of L_{xy} is $\approx 60\mu$m, which is significantly smaller than the mean transverse decay length of ≈ 1.1 mm expected for the signal. We require the proper decay length $\lambda > 100$ μm, where $\lambda = L_{xy}\frac{m_B}{\mathrm{p_T}(e\mu)}$, and m_B is the mass of the B_d^0 or B_s^0 meson. The efficiency of this requirement is studied using Monte Carlo simulation.

The pointing angle $\Delta\varphi$ is defined as the angle between $\vec{l}_{xy}$ and $\vec{\mathrm{p}}_\mathrm{T}(e\mu)$. For $e\mu$ pairs coming from the decay of a B, $\vec{l}_{xy}$ should point in the same direction as $\vec{\mathrm{p}}_\mathrm{T}(e\mu)$. Since we require $\lambda > 100$ μm, the direction of $\vec{l}_{xy}$ is well defined. The distribution of $\Delta\varphi$ for opposite-sign (OS) $B \to e^\pm\mu^\mp$ Monte Carlo events (signal) and for like-sign (LS) $e\mu$ events (background) with $5 < \mathrm{m}_{e\mu} < 6$ GeV/c^2 and $\lambda > 100$ μm is shown in Fig. 2A. We require $\Delta\varphi < 0.1$.

Due to the hard b-quark fragmentation, B mesons carry most of the transverse momentum of the b-quark and are isolated. The isolation is defined as $I = \frac{\mathrm{p_T}(e\mu)}{\mathrm{p_T}(e\mu)+\sum \mathrm{p_T}}$, where $\sum \mathrm{p_T}$ is the scalar sum of the transverse momenta of all tracks excluding the e and μ within a cone of $\Delta R < 1$ (where $\Delta R = \sqrt{(\Delta\eta)^2 + (\Delta\phi)^2}$)

around the momentum vector of the $e\mu$ pair. The z coordinate of these tracks at the closest approach to the beam line must be within 5 cm of the B candidate vertex to exclude tracks from other $p\bar{p}$ collisions that can occur during the same bunch crossing. We require $I > 0.7$. The efficiency of the isolation requirement is obtained using a data sample of fully reconstructed $B^{\pm} \to J/\psi K^{\pm}$ and $B^0 \to J/\psi K^{*0}$ events. The distribution of the isolation variable for (sideband subtracted) $B^{\pm} \to J/\psi K^{\pm}$ and $B^0 \to J/\psi K^{*0}$ events (signal) compared to the isolation of LS $e\mu$ events (background) with $5 < \mathrm{m}_{e\mu} < 6$ GeV/c^2 and $\lambda > 100$ μm is shown in Fig. 2B.

The λ, $\Delta\varphi$ and I requirements have been optimized by maximizing the signal-to-background significance, ϵ_S^2/ϵ_B, where ϵ_S is the efficiency for $B \to e^{\pm}\mu^{\mp}$ events, and ϵ_B is the efficiency for background events. To estimate ϵ_B we use LS $e\mu$ pairs in the 5 - 6 GeV/c^2 mass range as a sample of background.

Fully reconstructed $B \to e^{\pm}\mu^{\mp}$ events from a Monte Carlo simulation are used to estimate the mass resolution and the efficiency of the mass window requirements. We find a resolution of 33 MeV/c^2 and define the mass windows of 5.279$\pm$0.105 GeV/c^2 for the B_d^0 and 5.370$\pm$0.105 GeV/c^2 for the B_s^0. The uncertainty of the efficiency of the mass window requirement is estimated by varying the mass resolution by $\pm$10%.

Figure 1 shows the $\mathrm{m}_{e\mu}$distributions for OS and LS $e\mu$ pairs before and after the λ, $\Delta\varphi$ and I requirements. We observe 422 OS and 262 LS events for $5 < \mathrm{m}_{e\mu} < 6$ GeV/c^2 before the requirements, which is reduced to 85 OS and 58 LS events after the λ requirement, 16 OS and 12 LS events after the $\Delta\varphi$ requirement, and finally, 4 OS and 1 LS events after the I requirement. One OS event remains in the B_d^0 mass window, while no candidates are found in the B_s^0 mass window.

As there is no evidence for a signal we proceed to set limits. When setting limits we make no background subtraction and take into account the systematic uncertainties on the B_d^0 meson measured cross section (23%) [14], the efficiency and acceptance (10%), and the integrated luminosity (7%). We obtain $N^l(B_d^0 \to e^{\pm}\mu^{\mp})$ = 4.34(5.52) events and $N^l(B_s^0 \to e^{\pm}\mu^{\mp})$ = 2.52(3.38) events at 90 (95)% C.L., where N^l is the upper limit on the number of events. We determine the limits on $\mathcal{B}(B \to e^{\pm}\mu^{\mp})$ for B_s^0 and B_d^0 using the following relationship between N^l and the branching fraction:

$2 \cdot \sigma(B) \cdot \mathcal{B}(B \to e^{\pm}\mu^{\mp}) < \frac{N^l(B \to e^{\pm}\mu^{\mp})}{\int \mathcal{L}dt \cdot \epsilon_{tot}}$.

The factor of two takes into account that we do not distinguish B and $\bar{B}$ decays. We assume $\sigma(B_s^0) = 1/3 \times \sigma(B_d^0)$ [17], and use $\sigma(B_d^0)(\mathrm{p_T}(B) > 6$ GeV/c, $|y(B)| < 1.0) = 2.39 \pm 0.32 \pm 0.44$ μb [14], $\int \mathcal{L}dt = 102$ pb^{-1} and the total efficiency (ϵ_{tot}) value listed in Table I. We obtain the following upper bounds at 90(95)% C.L.:

$\mathcal{B}(B_s^0 \to e^{\pm}\mu^{\mp}) < 6.1(8.2) \times 10^{-6}$ and

$\mathcal{B}(B_d^0 \to e^{\pm}\mu^{\mp}) < 3.5(4.5) \times 10^{-6}$.

The relationship between the branching ratio $\mathcal{B}(B_s^0 \to$

$e^{\pm}\mu^{\mp}$) (similarly for the $\mathcal{B}(B_d^0 \to e^{\pm}\mu^{\mp})$ case) and the corresponding M_{LQ} is as follows [2]:

$$\Gamma(B_s^0 \to e\mu) = \pi\alpha_s^2(M_{LQ})\frac{1}{M_{LQ}^4}F_{B_s^0}^2 m_{B_s^0}^3 R^2$$

where:

$$R = \frac{m_{B_s^0}}{m_b}\left(\frac{\alpha_s(M_{LQ})}{\alpha_s(m_t)}\right)^{-\frac{4}{7}}\left(\frac{\alpha_s(m_t)}{\alpha_s(m_b)}\right)^{-\frac{12}{23}}$$

We use $F_{B_d^0} = 175 \pm 30$ MeV for the B_d^0 decay constant [18]. $F_{B_s^0}$ is derived from $F_{B_d^0}$ using the following relationship obtained from lattice QCD [18]: $F_{B_s^0}/F_{B_d^0} = 1.14 \pm 0.05$ resulting in $F_{B_s^0} = 200 \pm 35$ MeV. For the other quantities we use the PDG [19] values $m_{B_s^0} = 5.3696 \pm 0.0024$ GeV/c^2 for the B_s^0 meson mass, $m_{B_d^0} = 5.2792 \pm 0.0018$ GeV/c^2 for the B_d^0 meson mass, $m_b = 4.3 \pm 0.2$ GeV/c^2 for the b-quark mass, $\tau_{B_s^0} = 1.57 \pm 0.08$ ps for the B_s^0 lifetime, $\tau_{B_d^0} = 1.55 \pm 0.05$ ps for the B_d^0 lifetime, and $m_t = 175.9 \pm 6.9$ GeV/c^2 [20] for the top quark mass. We use $\alpha_s(M_Z) = 0.115$ which is evolved to M_{LQ} using the Marciano approximation [21], assuming no colored particles lie between m_t and M_{LQ}. We obtain the following lower bounds on the masses of the corresponding LQ at 90(95)% C.L.:

$M_{LQ}(B_s^0) > 20.7(19.3)$ TeV/c^2 and

$M_{LQ}(B_d^0) > 21.7(20.4)$ TeV/c^2.

The limits for the B_s^0 case and the theoretical prediction for $M_{LQ}(B_s^0)$ as a function of $\mathcal{B}(B_s^0 \to e^{\pm}\mu^{\mp})$ are shown in Fig. 3.

In conclusion we have searched for the decays $B_s^0 \to e^{\pm}\mu^{\mp}$ and $B_d^0 \to e^{\pm}\mu^{\mp}$. No evidence is found for these decays. We set upper limits on the branching fractions and lower limits on the corresponding Pati-Salam leptoquark masses.

ACKNOWLEDGMENTS

We thank S. Willenbrock for motivating us to do this analysis and for his contribution to the theoretical interpretation. We thank the Fermilab staff and the technical staffs of the participating institutions for their vital contributions. This work was supported by the U.S. Department of Energy and National Science Foundation; the Italian Istituto Nazionale di Fisica Nucleare; the Ministry of Education, Science and Culture of Japan; the Natural Sciences and Engineering Research Council of Canada; the National Science Council of the Republic of China; the Swiss National Science Foundation; and the A. P. Sloan Foundation.

[1] J. Pati and A. Salam, Phys. Rev. D **10**, 275 (1974).
[2] G. Valencia, S. Willenbrock, Phys. Rev. D **50**, 6843 (1994).
[3] A.V. Kuznetsov and N.V. Mikheev, Phys. Lett. B **329**, 295 (1994).
[4] M. Acciarri *et al.*, Phys. Lett. B **391**, 474 (1997).
[5] R. Ammar *et al.*, Phys. Rev. D **49**, 5701 (1994).
[6] F. Abe *et al.*, Nucl. Inst. and Meth. A **271**, 387 (1988).
[7] D. Amidei *et al.*, Nucl. Instrum. Meth. **A350**, 73 (1994).
[8] In CDF the positive z (longitudinal) axis lies along the proton beam direction, r is the radius from this axis, θ is the polar angle and ϕ is the azimuthal angle. Pseudorapidity (η) is defined as $\eta \equiv -\ln(\tan(\theta/2))$. E_T and p_T are the energy flow and the momentum measured transverse to the beam line, respectively.
[9] The impact parameter is the distance of closest approach of the track helix to the beam axis, measured in the transverse plane.

[10] G.W. Foster et. al., Nucl. Inst. and Meth. A **269**, 93 (1988).
[11] P. Nason, S. Dawson, R. Ellis, Nucl. Phys. B **326**, 49 (1988); P. Dawson *et al.*, Nucl. Phys. B **327**, 49 (1988); M. Mangano *et al.*, Nucl. Phys. B **373**, 295 (1992).
[12] A. Martin, R. Roberts, J. Stirling, Phys. Rev. D **47**, 867 (1993).
[13] C. Peterson *et al.*, Phys. Rev. D **27**, 105 (1983).
[14] F. Abe *et al.*, Phys. Rev. Lett. **75**, 1451 (1995).
[15] F. Abe *et al.*, Phys. Rev. D **8** , 072001 (1998).
[16] F. Abe *et al.*, Phys. Rev. D **52**, 2624 (1995).
[17] 1/3 is consistent with the measurement of $0.34 \pm 0.10 \pm 0.03$: F. Abe *et al.*, Phys. Rev. D **54**, 6596 (1996).
[18] C. Bernard, Review talk given at 7th International Symposium on Heavy Flavor Physics, Santa Barbara, CA, 7-11 July 1997, hep-ph/9709460 and references therein.
[19] R.M. Barnett et al., Phys. Rev. D **54**, 1 (1996) and 1997 off-year partial update for the 1998 edition available on the PDG WWW pages (URL: http://pdg.lbl.gov/).
[20] F. Abe *et al.*, Phys. Rev. Lett. **80**, 2767 (1998).
[21] W. Marciano, Phys. Rev. D **29**, 580 (1984).

TABLE I. Efficiencies and their uncertainties (statistical and systematic uncertainties are added in quadrature). The total efficiency is the product of the individual efficiencies when applied in that order.

Requirement	Efficiency in %
Geometric and kinematic acceptance for $p_T(B) > 6$ GeV/c and rapidity $\|y(B)\| < 1$	2.27 ± 0.024
Trigger efficiency	37.2 ± 1.6
Reconstruction of two tracks in CTC	89.8 ± 3.6
Muon selection criteria	99.5 ± 0.1
Electron selection criteria	84.8 ± 1.1
Track and vertex quality selection criteria	68.3 ± 3.1
Proper decay length ($\lambda > 100\mu m$)	81.0 ± 0.8
Pointing angle ($\Delta\varphi < 0.1$)	85.2 ± 2.3
Isolation ($I > 0.7$)	85.1 ± 3.0
Mass window	98.0 ± 0.6
Total efficiency $\times$ acceptance (ϵ_{tot})	0.252 ± 0.022

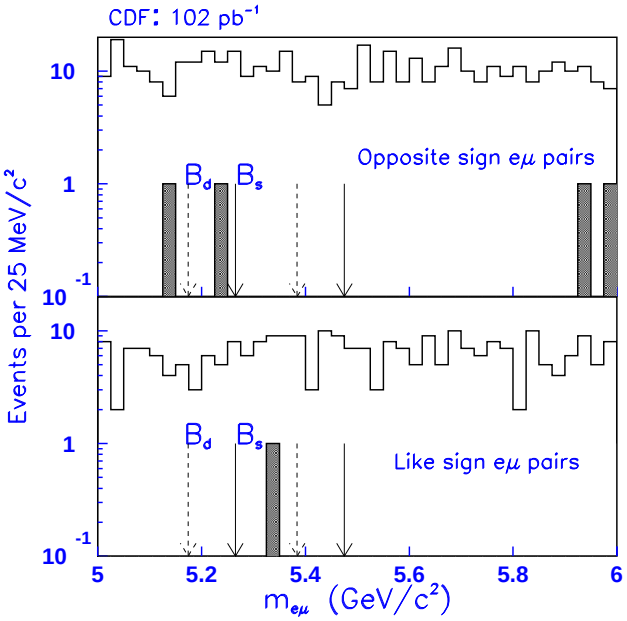

FIG. 1. Invariant mass distribution of OS and LS $e\mu$ pairs before and after the λ, $\Delta\varphi$ and I requirements. The arrows indicate the mass windows for B_d^0 (5.279±0.105 GeV/c^2) and B_s^0 (5.370±0.105 GeV/c^2).

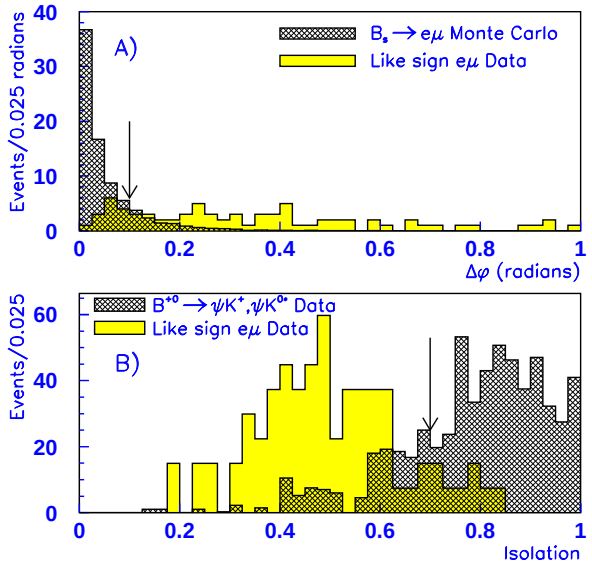

FIG. 2. A) Distribution of the pointing variable $\Delta\varphi$ for Monte Carlo events (signal) and for LS eμ-events (background) with $5 < m_{e\mu} < 6$ GeV/c^2 and $\lambda > 100$ μm. B) Distribution of the isolation variable for sideband subtracted $B^{\pm} \to J/\psi K^{\pm}$ and $B^0 \to J/\psi K^{*0}$ events (signal) compared to the isolation of LS eμ-events (background) with $5 < m_{e\mu} < 6$ GeV/c^2 and $\lambda > 100$ μm. The arrows in both cases indicate the cut values. In both plots the two distributions are normalized to the same total number of entries.

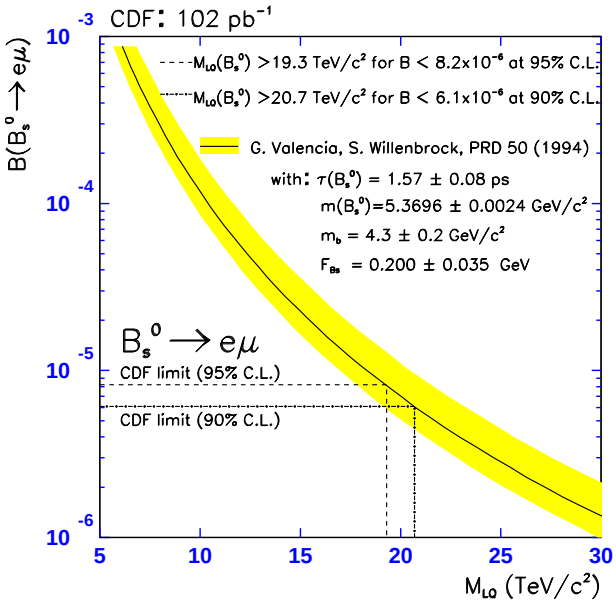

FIG. 3. Pati-Salam leptoquark mass limits corresponding to the 90(95)% C.L. limits on $\mathcal{B}(B_s^0 \to e^{\pm}\mu^{\mp})$. The error band represents the theoretical uncertainties.